Original Article

Prediction of visceral pleural invasion of clinical stage IA lung adenocarcinoma based on computed tomography features

Deng Lyu[1#^], Yun Wang[1#^], Wenting Tu[1#^], Su Hu[2], Yanqing Ma[3], Xiuxiu Zhou[1^], Yi Xiao[1^], Rongbo Dong[4], Li Fan[1^], Shiyuan Liu[1^]

[1]Department of Radiology, Second Affiliated Hospital of Navy Medical University, Shanghai, China; [2]Department of Radiology, The First Affiliated Hospital of Soochow University, Suzhou, China; [3]Department of Radiology, Zhejiang Provincial People's Hospital, Affiliated People's Hospital of Hangzhou Medical College, Hangzhou, China; [4]Department of Radiology, The 95829 Army Hospital of PLA, Wuhan, China

Contributions: (I) Conception and design: D Lyu, Y Wang, R Dong, L Fan, S Liu; (II) Administrative support: R Dong, L Fan, S Liu; (III) Provision of study materials or patients: D Lyu, Y Wang, Y Ma, S Hu; (IV) Collection and assembly of data: D Lyu, Y Wang, W Tu, X Zhou, Y Xiao; (V) Data analysis and interpretation: D Lyu, Y Wang, W Tu, R Dong, L Fan; (VI) Manuscript writing: All authors; (VII) Final approval of manuscript: All authors.

[#]These authors contributed equally to this work.

Correspondence to: Rongbo Dong, MD. Department of Radiology, The 95829 Army Hospital of PLA, 15 Gongnongbing Road, Jiang'an District, Wuhan 430012, China. Email: apollodong@163.com; Li Fan, MD; Shiyuan Liu, MD. Department of Radiology, Second Affiliated Hospital of Navy Medical University, 415 Fengyang Road, Huangpu District, Shanghai 200003, China. Email: fanli0930@163.com; radiology_cz@163.com.

Background: In lung cancer, preoperative prediction of visceral pleural invasion (VPI) is helpful for choosing the best treatment plan and improving the prognosis of patients. This study aimed to investigate the usefulness of computed tomography (CT) features in predicting VPI in clinical stage IA peripheral lung adenocarcinoma (LUAD) with pleural contact.

Methods: This study divided the type of contact between tumor and pleura into indirect and direct contacts. This study retrospectively analyzed patients with clinical stage IA peripheral LUAD in three hospitals and enrolled 485 patients. The CT features of lesions were analyzed to predict VPI, including relative pleural features, tumor signs, and characteristics between the tumor and pleura. Univariate and multivariate logistic regression analyses were used to select the best combination of variables to predict VPI, and the prediction models were developed.

Results: The multivariate logistic regression analysis identified solid component size, pleural tag type, and vascular convergence sign to be independent risk factors for VPI in indirect pleural contact type. The area under curve (AUC) values of the model for predicting VPI in the training, internal validation, and external validation sets were 0.887, 0.799, and 0.862, respectively. Solid component size and pleural indentation sign were identified as independent risk factors for predicting VPI in direct pleural contact type. The AUC values of the model for predicting VPI in the training, internal validation, and external validation sets were 0.903, 0.848, and 0.842, respectively.

Conclusions: CT predictors associated with VPI differ based on the type of contact with the pleura. The multivariate logistic regression models utilizing CT features demonstrates acceptable diagnostic accuracy in predicting VPI in clinical stage IA LUAD with pleural contact.

Keywords: Lung cancer; adenocarcinoma; visceral pleural invasion (VPI); computed tomography (CT); prediction

Submitted Oct 19, 2024. Accepted for publication Jan 27, 2025. Published online Mar 27, 2025.
doi: 10.21037/tcr-24-2015
View this article at: https://dx.doi.org/10.21037/tcr-24-2015

^ ORCID: Deng Lyu, 0000-0002-2205-6107; Yun Wang, 0000-0001-8914-9861; Wenting Tu, 0000-0003-1010-7189; Xiuxiu Zhou, 0000-0003-2405-0566; Yi Xiao, 0000-0002-3212-2892; Li Fan, 0000-0003-4722-3933; Shiyuan Liu, 0000-0003-3420-0310.

Introduction

Lung cancer is one of the malignant tumors with the highest incidence and mortality rates, according to the 2023 Burden of Cancer Disease Report in China (1). Additionally, lung adenocarcinoma (LUAD) is the most prevalent pathological subtype of non-small cell lung cancer (1). Visceral pleural invasion (VPI) is a significant adverse prognostic indicator in lung cancer, defined as tumor infiltration extending beyond the elastic fiber layer of the visceral pleura (2).

Because of the abundant lymphatic ducts (lymphatic reflux system) in the visceral pleura, which communicate with the axial lymphatic system that accompanies the trachea, bronchus, and blood vessels, lung cancer with VPI is more likely to have hilar and mediastinal lymph node metastasis through the axial lymphatic system (3) Additionally, it is independently associated with the skipping N2 lymph node metastasis (4). Therefore, patients often need adjuvant chemotherapy after surgery (5).

Highlight box

Key findings

- Computed tomography (CT) predictors associated with visceral pleural invasion (VPI) differ based on the type of contact with the pleura. The multivariate logistic regression models utilizing CT features demonstrates acceptable diagnostic accuracy in predicting VPI in clinical stage IA lung adenocarcinoma (LUAD) with pleural contact.

What is known and what is new?

- Lung cancer with no contact with pleura and presenting as pure ground glass nodules do not invade the visceral pleura.
- According to the type of contact between the tumor and the pleura, the CT signs of the related pleural, the characteristics between the tumor and the pleura, and the features of the tumor were comprehensively analyzed, new signs such as density changes in pleural indentation area were included, the risk factors were explored, and the prediction model was constructed and validated.

What is the implication, and what should change now?

- When evaluating whether VPI occurs in clinical stage IA LUAD with pleural contact, attention should be paid to the solid component size. For LUAD in indirect contact with the pleura, when preoperative CT indicates the Peacock-tail sign, vascular convergence sign and emphysema background, the possibility of VPI should be considered. For LUAD in direct contact with the pleura, attention should be paid to whether there is a pleural tags sign, a solid component touching the pleura, or an indentation in the adjacent pleura. However, it should be noted that interlobar pleura indentation and the density changes in the pleural indentation area do not necessarily indicate VPI.

Pathological VPI in cT1N0M0 LUAD results in an upgrade of the T stage from T1 to T2 and the TNM stage from IA to IB according to the 8th edition of TNM staging criteria (2). Recent research has demonstrated that in patients with clinical stage T1 lung cancer with an invasion of the visceral pleura, lobectomy may lead to an improved prognosis (6). Patients with T1-sized and VPI-positive lung cancer require more extensive lymph node dissection than lymph node sampling (7). Consequently, surgeons must accurately determine the VPI status of patients with tolerable pulmonary function reserve to make appropriate treatment decisions.

The intrinsic invasiveness of the tumor is essential in determining its potential to invade the visceral pleura. Previous studies have reported that pure ground glass nodules (pGGNs) do not invade the visceral pleura because of their limited invasiveness, which hinders the penetration of the internal elastic layer of the pleura (8-13). Additionally, assessing the spatial relationship between the tumor and the pleura is crucial in determining the likelihood of VPI. Lung cancer that does not interact with the pleura does not invade the visceral pleura (8,13). Accordingly, this study analyzed lesions that came in contact with the pleura, excluding pGGNs, and categorized the relationship between tumors and the pleura as direct or indirect. Different indicators were evaluated for each group, and logistic regression was used to identify the best predictors for each type of lesion. Furthermore, this study incorporated new CT indicators, including density characteristics in the area where the lesion makes contact with the pleura, which had not been analyzed in previous studies. While several studies have explored the use of radiomics and deep learning for VPI prediction, challenges, including the limited generalizability and interpretability of current models, hinder their clinical utility (14-16).

Consequently, a comprehensive analysis was conducted on the relative pleural features, tumor signs, and characteristics of the tumor and pleura, which can be readily assessed in routine clinical practice, to investigate the risk factors associated with VPI, construct predictive models, and evaluate their predictive utility in internal and external validation sets. This analysis will provide the basis for the preoperative evaluation of VPI in LUAD based on traditional CT features, which may provide valuable information for clinical treatment decisions. We present this article in accordance with the TRIPOD reporting checklist (available at https://tcr.amegroups.com/article/view/10.21037/tcr-24-2015/rc).

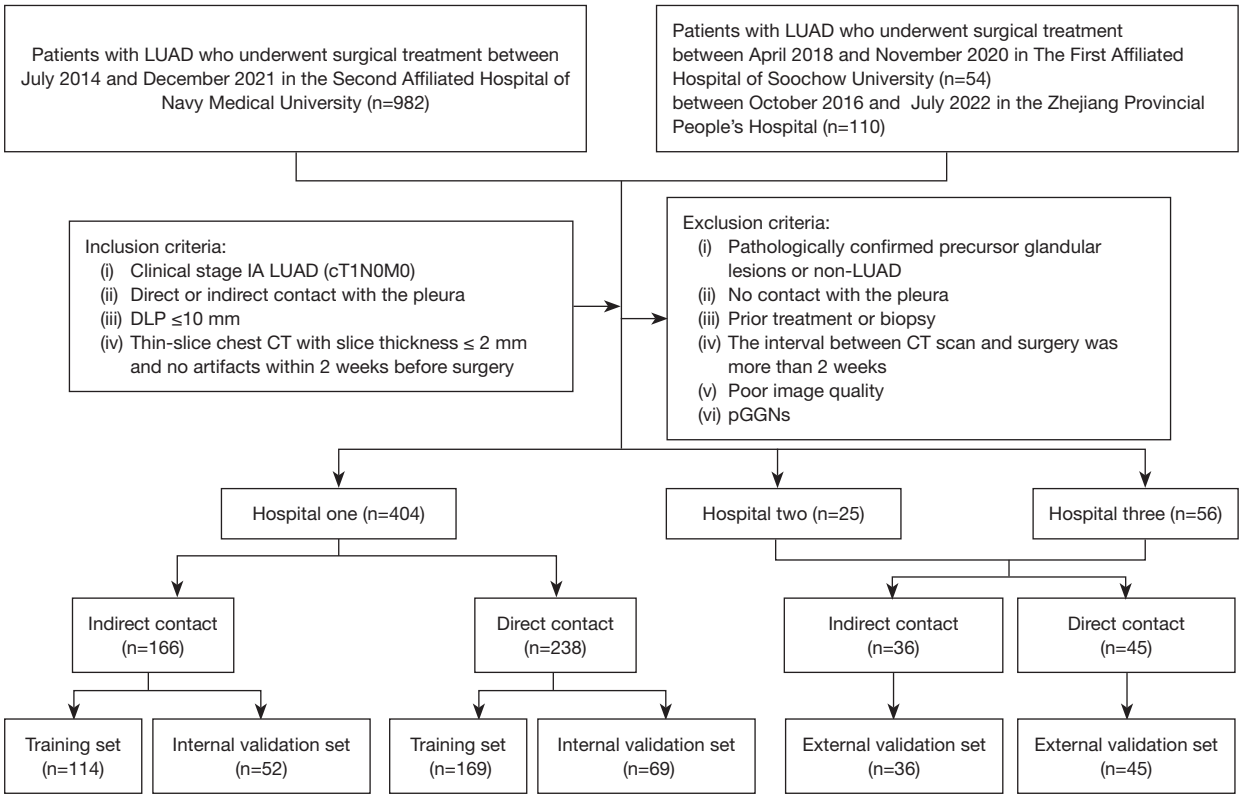

Figure 1 The flowchart of inclusion and exclusion criteria of patients. CT, computed tomography; DLP, distance between the lesion and the pleura; LUAD, lung adenocarcinoma; pGGNs, pure ground glass nodules.

Methods

Patients

This study retrospectively analyzed the clinical and imaging data of patients with peripheral lung cancer who underwent preoperative chest CT examination and were confirmed during surgery and pathological examination in three hospitals. Herein, 116 patients with pGGNs who were in contact with the pleura were analyzed retrospectively, and none exhibited pathological VPI. Thus, such lesions were excluded. The inclusion criteria were as follows: (I) patients with clinical stage IA (cT1N0M0) LUAD; (II) Patients with preoperative CT that revealed that the tumor was located under the pleura, directly or indirectly in contact with the pleura. Indirect contact was defined as a certain distance between the tumor and the pleura, connected by one or more linear or strip shadows (pleural tags sign). Direct contact was defined as the tumor in direct contact with the pleura. (III) Patients in which the minimum distance between the lesion and the pleura (DLP) was ≤10 mm; (IV) patients that underwent chest CT with a thin slice thickness of ≤2 mm within 2 weeks before surgery. The exclusion criteria were as follows: (I) patients with precursor glandular lesions or non-LUAD confirmed using pathology examination; (II) patients with a lesion that is not in contact with the pleura; (III) patients with previous treatment or biopsy; (IV) patients in whom the interval between CT scan and surgery was >2 weeks; (V) patients with poor CT image quality (with artifacts or slice thickness >2 mm); (VI) patients with pGGNs. We included 404 eligible patients in the Second Affiliated Hospital of Navy Medical University as an internal dataset, including 166 patients with indirect contact type and 238 patients with direct contact type. All patients were divided into a positive group and a negative group based on the VPI status reported by pathologists. The patients with the two types in the internal dataset were randomly divided into the training set and the internal validation set at a ratio of 7:3. A total of 81 patients were diagnosed in The First Affiliated Hospital of Soochow University (n=25) and the Zhejiang Provincial People's Hospital (n=56) were included as an external validation set, including 36 patients with indirect contact type and 45

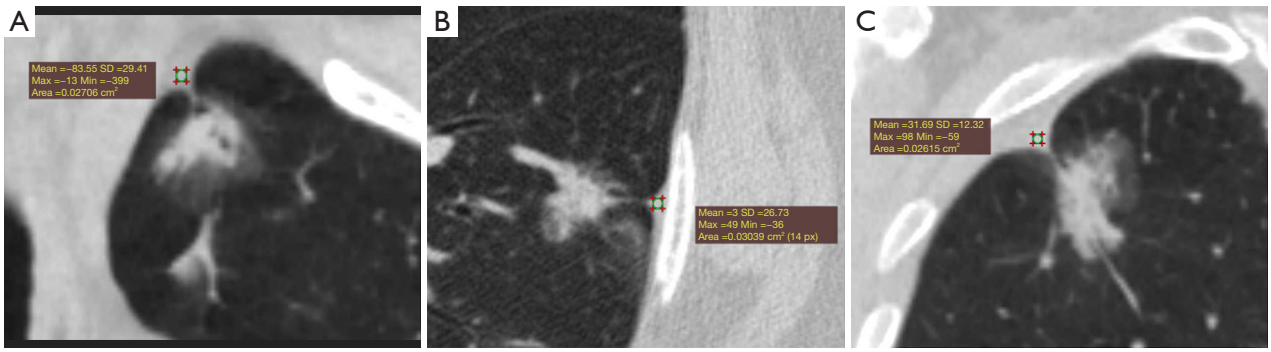

Figure 2 The density changes of the pleura in indirect pleural contact type. (A) A 76-year-old man presented with mGGNs in the left upper lobe and fat density in the mediastinal pleural indentation (Type C). (B) A 54-year-old female presented with mGGNs in the left lower lobe and water density in the costal pleural indentation (Type D). (C) A 57-year-old female presented with mGGNs in the right upper lobe and soft tissue density in the costal pleural indentation (Type E). SD in figures means standard deviation of CT value. CT, computed tomography; mGGNs, mixed ground glass nodules.

patients with direct contact type. *Figure 1* illustrates the detailed patient inclusion procedure.

The study was conducted in accordance with the Declaration of Helsinki (as revised in 2013) and approved by the Ethics Committee of the Second Affiliated Hospital of Navy Medical University (No. CZ-20210528-01). The other hospitals were informed and agreed to the study. Individual consent for this retrospective analysis was waived.

Equipment and parameters

For detailed scanning equipment and parameters, refer to Appendix 1.

CT image measurement and evaluation

The DICOM images of the patients were imported into Radiant DICOM Viewer software (version 4.2.1, Medixant, Poland), and the CT features of the lesions were displayed using multiplanar reconstruction (MPR) and maximum intensity projection (MIP). The quantitative and qualitative evaluation of the lesions was performed by two radiologists with >7 years of experience. Quantitative parameter evaluation: The mean value of measurements by the two radiologists was used as the final result. Qualitative indicator evaluation: the signs of lesions were interpreted by two radiologists using a double-blinded method, disagreements were discussed until a consensus was reached.

First, relative pleural features were evaluated. The pleural indentation sign was qualitatively analyzed, and subgroup analysis was performed between the interlobar and non-interlobar pleura groups (costal pleura, mediastinal pleura, and diaphragmatic pleura). The density changes of the pleura were analyzed and classified (*Figures 2,3*).

Second, tumor signs were evaluated, tumor size and solid component size were measured quantitatively, and the consolidation-to-tumor ratio (CTR) was calculated. Qualitative analysis was performed for tumor location, density type (mixed ground glass nodule or solid nodule), shape (round/oval or irregular shape), tumor-lung interface (well-defined or ill-defined), margin (lobulation and spiculation), internal morphology change (vacuole sign and cavity or cystic airspace), adjacent features (bronchial change and vascular convergence sign) and emphysema background [emphysema in the lobe of lung cancer (ELLC)].

Third, the characteristics of the tumor and the pleura were evaluated. For tumors in indirect contact with the pleura, the minimum vertical DLP was measured on MPR images at the lung window, the presence of the bridge sign was qualitatively analyzed, and the morphology of the pleural tags sign was classified (*Figure 4*). For tumors in direct contact with the pleura, the longest interface length of the whole tumor and solid component was measured by drawing a straight line at the lung window on MPR images, and the ratio of the longest interface length of the whole tumor to the tumor size was calculated. The presence or absence of solid components contacting the pleura and the combination of pleural tags signs were analyzed qualitatively. The type of direct contact between the tumor and the pleura was classified based on the proportion of

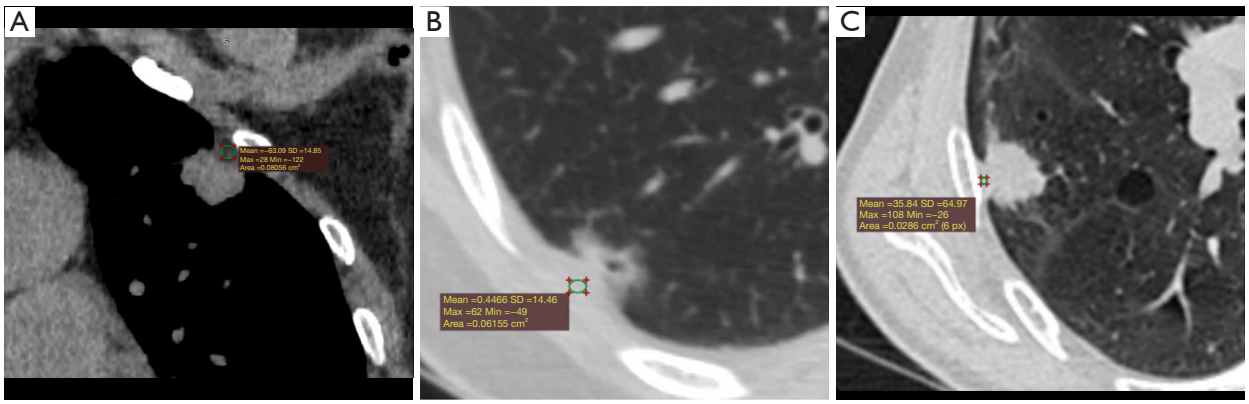

Figure 3 The density changes of the pleura in direct pleural contact type. (A) A 59-year-old female presented with solid nodule in the left upper lobe and fat density in the costal pleural indentation (Type C). (B) A 55-year-old female presented with mGGNs in the right lower lobe and water density in the costal pleural indentation (Type D). (C) A 64-year-old man presented with solid nodule in the right upper lobe and soft tissue density in the costal pleural indentation (Type E). SD in figures means standard deviation of CT value. CT, computed tomography; mGGNs, mixed ground glass nodules.

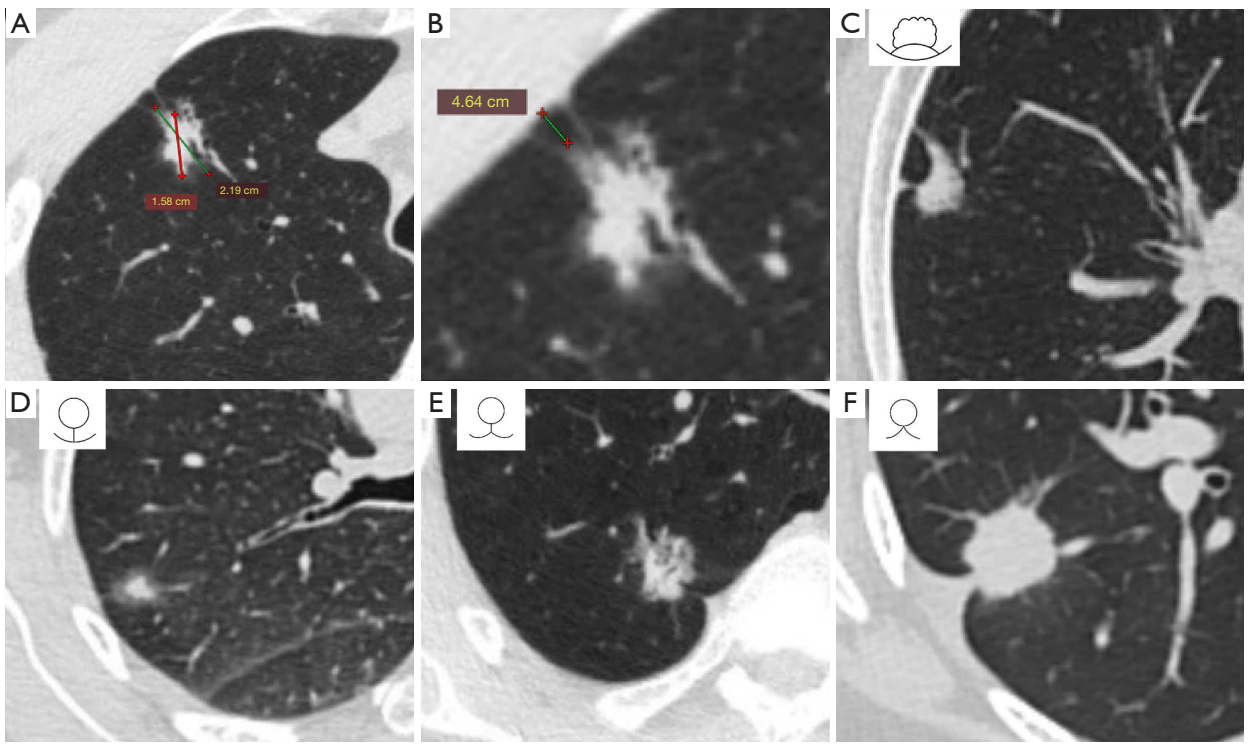

Figure 4 The characteristics of the tumor and the pleura in indirect pleural contact type. (A,B) A 53-year-old man presented with mGGNs in the right upper lobe and tumor size is 21.9 mm (green line), solid component size is 15.8 mm (red line), and minimum vertical DLP is 4.64 mm. (C) A 43-year-old man presented with mGGNs in the right upper lobe and the edge of the tumor was flat and deformed, showing an arch bridge, which was the bridge sign, the line drawing on the upper left in (C) is the interpretation the bridge sign. (D) The tumor was connected to the pleura by thin line, without pleural indentation sign, which was the Rat-tail sign (Type I). (E) The tumor was connected to the pleura by the thin line with pleural indentation sign, which was the Fish-tail sign (Type II). (F) The tumor was connected to the pleura by a thick strip with pleural indentation sign, which was the Peacock-tail sign (Type III). The line drawings on the upper left in (D-F) are the interpretation of the classification of pleural tags sign. DLP, distance between the lesion and the pleura; mGGNs, mixed ground glass nodules.

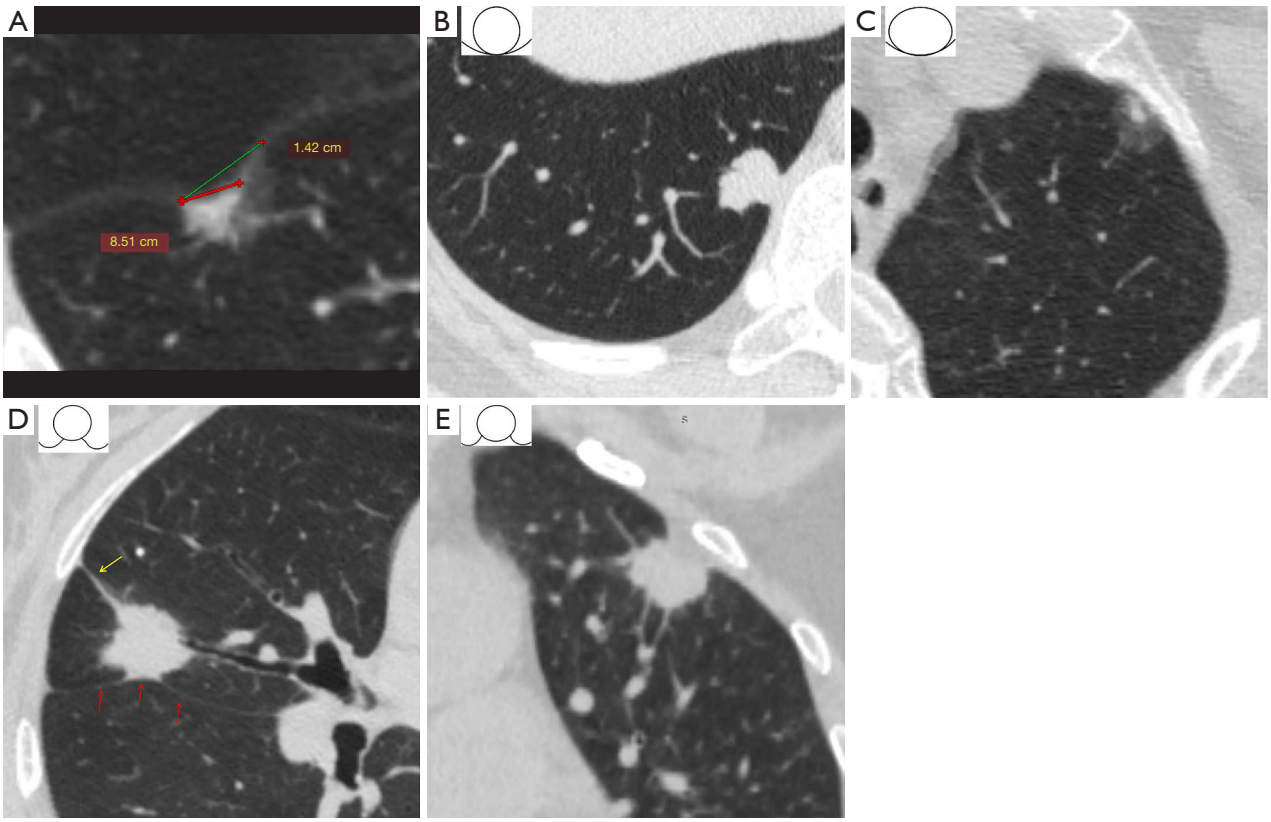

Figure 5 The characteristics of the tumor and the pleura in direct pleural contact type. (A) A 64-year-old man presented with mGGNs in the right lower lobe and direct contact with the interlobar fissure with pleural indentation, with solid components contacting the pleura, the whole tumor contact length is 14.2 mm (green line), solid component contact length is 8.51 mm (red line). (B) A 49-year-old female presented with solid nodule in the right lower lobe, which directly contacted the adjacent costal pleura with a narrow base without pleural indentation, and the overall proportion of tumor contacting pleura was 47.62% (Type I). (C) A 73-year-old female presented with mGGNs in the left upper lobe, which directly contacted the adjacent costal pleura with a wide base without pleural indentation, and the overall proportion of tumor contacting pleura was 92.03% (Type II). (D) A 57-year-old female presented with solid nodule in the right middle lobe, which directly contacted the adjacent interlobar pleura with a narrow base with pleural indentation (red arrows), and the overall proportion of tumor contacting pleura was 38.29% (Type III). The tumor was associated with pleural tags sign (yellow arrow). (E) A 59-year-old female presented with solid nodule in the left upper lobe, which directly contacted the adjacent costal pleura with a wide base with pleural indentation, and the overall proportion of tumor contacting pleura was 55.35% (Type VI). The line drawings on the upper left in (B-E) are the interpretation of the classification based on the proportion of tumors contacting the pleura and pleura morphology. mGGNs, mixed ground glass nodules.

the longest interface length of the whole tumor and the morphology change of the pleura (*Figure 5*). The definitions of CT features are described in Table S1.

Pathological diagnosis

All pathological results were obtained from the official pathology report issued the Second Affiliated Hospital of Navy Medical University, for detailed pathological diagnosis, refer to Appendix 2.

Statistical analysis

SPSS 20.0 software and R statistical software (R version 4.2.2) were used for data analysis, for detailed pathological diagnosis, refer to Appendix 3.

Table 1 Classification based on the shape of pleural tags sign in indirect pleural contact type

Group	Type I	Type II	Type III	P value
VPI-negative	28 (43.1)[a]	30 (46.1)[b]	7 (10.8)[c]	<0.001
VPI-positive	3 (6.1)[a]	25 (51.0)[b]	21 (42.9)[c]	

"a, b, and c" represent a subset of the classification based on the pleural tags sign, with the same letter indicating that they are not significantly different from each other at the P<0.05 level. Data are presented as n (%). VPI, visceral pleural invasion.

Table 2 Classification based on the proportion of tumors contacting the pleura and pleura morphology in direct pleural contact type

Group	Type I	Type II	Type III	Type IV	P value
VPI-negative	8 (9.5)[a,b]	30 (35.7)[b]	10 (11.9)[a,b]	36 (42.9)[a]	0.03
VPI-positive	6 (7.1)[a,b]	15 (17.6)[b]	9 (10.6)[a,b]	55 (64.7)[a]	

"a, b" represent a subset of the classification based on the proportion of tumors contacting the pleura and pleura morphology, with the same letter indicating that they are not significantly different from each other at the P<0.05 level. Data are presented as n (%). VPI, visceral pleural invasion.

Results

Clinicopathological characteristics

For tumors with indirect contact with the pleura, 89 and 113 patients were VPI positive and VPI negative, respectively. There were 49 VPI-positive and 65 VPI-negative patients in the training set. The results demonstrated that the pathological grade of LUAD in the training set was statistically different between the two groups (P<0.05), see Table S2.

For tumors with direct contact with the pleura, 138 and 145 patients were VPI positive and VPI negative, respectively. The training set comprised 85 VPI-positive and 84 VPI-negative patients. In the training set, the difference in age between the two groups was statistically significant (P<0.05). Patients in the VPI-positive group were older than those in the VPI-negative group. The pathological grade of LUAD in the training and internal validation sets was statistically significant between the two groups (P<0.05), see Table S3.

Inter-observer consistency analysis

Based on the evaluation of indirect contact type lesions, the inter-observer agreement of quantitative parameters measured in the internal and external sets was good (ICC =0.887–0.972), and the consistency of qualitative indicators was strong (Kappa value =0.823–1.000) (Table S4). Based on the evaluation of direct contact type lesions, the inter-observer agreement of quantitative parameters measured in the internal and external sets was good (ICC =0.941–0.993), and the consistency of qualitative indicators was strong (Kappa value =0.825–1.000) (Table S5).

Relationship between tumor and pleura

Subgroup analysis of pleural indentation sign between interlobar and non-interlobar pleura groups

No significant difference was observed in the pleural indentation sign between the VPI positive and VPI negative groups in the interlobar pleura group (P>0.05), irrespective of the type of contact between the tumor and pleura. The pleural indentation sign in the non-interlobular pleura group was more common in the VPI-positive group, and the difference was statistically significant (P<0.05). Tables S6,S7 illustrate the detailed analysis.

Classification based on the morphology and density changes of the pleura

No significant difference in density change classification in the pleural indentation area between the VPI positive and VPI negative groups (P>0.05), irrespective of the type of contact between the tumor and pleura. Tables S8,S9 illustrate the detailed analysis.

Classification based on the shape of pleural tags sign

For tumors with indirect contact with the pleura, the Chi-square test revealed that the pairwise comparison of the three types was statistically significant (χ^2=35.939, P<0.001). *Table 1* illustrates that the proportion of VPI-positive tumors with the peacock-tail sign was the highest.

Classification based on the proportion of tumors contacting the pleura and pleura morphology

For tumors with direct contact with the pleura, the Chi-square test and pairwise comparison revealed that types II and VI were statistically different (χ^2=9.300, P=0.03) (*Table 2*), indicating that the pleural indentation sign was a more important factor in predicting VPI than the proportion of tumors that make contact with the pleura.

Univariate and multivariate analysis

For tumors with indirect contact with the pleura, univariate analysis revealed that there were statistically significant

Table 3 Univariate and multivariate logistic regression analysis of factors in indirect pleural contact type

Factors	Univariate logistic regression analysis		Multivariate logistic regression analysis	
	OR (95% CI)	P value	OR (95% CI)	P value
Tumor size (mm)	1.12 (1.04–1.21)	0.003	–	–
Solid component size (mm)	1.19 (1.10–1.28)	<0.001	1.12 (1.03–1.22)	0.01
CTR (%)	1.04 (1.02–1.05)	<0.001	–	–
Density type	2.75 (1.10–7.19)	0.03	–	–
Spiculation sign	4.67 (1.94–12.00)	0.001	–	–
Vascular convergence sign	19.95 (5.33–130.44)	<0.001	9.53 (2.27–66.21)	0.006
Emphysema background	10.67 (1.81–203.17)	0.03	6.34 (0.72–149.5)	0.14
Bridge sign	3.89 (1.33–13.06)	0.02		
Pleural tag sign type	3.04 (1.93–5.32)	<0.001	2.36 (1.39–4.45)	0.003

OR, odds ratio; CI, confidence interval; CTR, consolidation-to-tumor ratio.

differences in tumor size, solid component size, CTR, density type, pleural tags sign type, bridge sign, spiculation sign, vascular convergence sign, emphysema background between VPI positive and VPI negative patients with LUAD (P<0.05) (Table S10), after removing the multicollinearity factor (Table S11). Multivariate logistic regression analysis revealed that the solid component size [odds ratio (OR) =1.12], the type of pleural tags sign (OR =2.36), and vascular convergence sign (OR =9.53) were independent risk factors for VPI. Multivariate logistic regression analysis was used to select the best predictors to construct the model. The best predictors included solid component size, vascular convergence sign, emphysema background, and pleural tags sign, as presented in *Table 3*.

For tumors with direct contact with the pleura, univariate analysis revealed that statistically significant differences were observed in age, tumor size, solid component size, CTR, whole tumor contact length, solid component contact length, density type, solid component contact pleura, pleural indentation sign, pleural tags sign, spiculation sign, bronchial change, vascular convergence sign, and emphysema background between VPI positive and VPI negative patients with LUAD (P<0.05) (Table S12), after removing the multicollinearity factor (Table S13). Multivariate logistic regression analysis revealed that solid component size (OR =1.28) and pleural indentation sign (OR =2.73) were independent risk factors for VPI. Multivariate logistic regression analysis was used to select the best predictors to construct the model. The best predictors included solid component size, pleural indentation, pleural tags, and solid component attachment signs (*Table 4*).

Regarding the predictive efficacy of the model. For tumors with indirect contact with the pleura, with 0.435 as the best cut-off value, the accuracy, sensitivity, specificity, and AUC of the model in the training set were 82.46%, 83.67%, 81.54%, and 0.887. On the internal validation set, the accuracy was 78.84%, the sensitivity was 72.41%, the specificity was 86.96%, and the AUC was 0.799; on the external validation set, the accuracy was 88.89%, the sensitivity was 72.73%, the specificity was 96.00%, the AUC value was 0.862, as presented in *Table 5*. For tumors with direct contact with the pleura, with 0.643 as the best cut-off value, the accuracy, sensitivity, specificity, and AUC of the model in the training set were 82.25%, 75.29%, 89.29%, and 0.903. On the internal validation set, the accuracy was 76.81%, the sensitivity was 90.32%, the specificity was 65.79%, and the AUC was 0.848. On the external validation set, the accuracy was 80.00%, the sensitivity was 81.82%, the specificity was 78.26%, and the AUC value was 0.842 (*Table 5*).

Discussion

Based on previous studies and the actual case collection, this study excluded two types of tumors that clearly did not invade the visceral pleura on CT: lesions without contact with the pleura and pGGNs. All the included patients developed lesions with potential invasion of the visceral pleura. Compared with previous studies, this study made iterative modifications to the inclusion criteria. Thus, the prediction model was constructed, and its prediction

Table 4 Univariate and multivariate logistic regression analysis of factors in direct pleural contact type

Factors	Univariate logistic regression analysis		Multivariate logistic regression analysis	
	OR (95% CI)	P value	OR (95% CI)	P value
Age (years)	1.03 (1.00–1.07)	0.057	–	–
Tumor size (mm)	1.23 (1.14–1.32)	<0.001	–	–
Solid component size (mm)	1.32 (1.23–1.44)	<0.001	1.28 (1.18–1.42)	<0.001
CTR (%)	1.06 (1.04–1.08)	<0.001	–	–
Density type	16.96 (6.33–59.22)	<0.001	–	–
Shape	0.55 (0.27–1.09)	0.09	–	–
Spiculation	16.17 (6.03–56.49)	<0.001	–	–
Bronchial change	1.88 (1.01–3.53)	0.049	–	–
Vascular convergence sign	4.44 (1.35–20.04)	0.03	–	–
Emphysema background	5.47 (1.39–36.32)	0.03	–	–
Pleural indentation sign	2.52 (1.32– 4.90)	0.006	2.73 (1.06–7.43)	0.041
Pleural tags sign	7.26 (3.73–14.65)	<0.001	1.92 (0.78–4.71)	0.15
Solid component contact pleura	39.79 (8.11–719.78)	<0.001	4.68 (0.73–92.53)	0.17
Whole tumor contact length	1.10 (1.04–1.16)	<0.001	–	–
Solid component contact length	1.29 (1.20–1.41)	<0.001	–	–

OR, odds ratio; CI, confidence interval; CTR, consolidation-to-tumor ratio.

Table 5 The predictive efficacy of multivariate logistic regression model with pleural contact

Data set	Cut-off	AUC (95% CI)	Accuracy (%)	Sensitivity (%)	Specificity (%)	PPV (%)	NPV (%)
Indirect contact							
Training	0.435	0.887 (0.814–0.939)	82.46	83.67	81.54	77.36	86.88
Internal validation		0.799 (0.665–0.897)	78.84	72.41	86.96	87.50	71.43
External validation		0.862 (0.706–0.954)	88.89	72.73	96.00	88.89	88.89
Direct contact							
Training	0.643	0.903 (0.848–0.943)	82.25	75.29	89.29	87.67	78.13
Internal validation		0.848 (0.742–0.923)	76.81	90.32	65.79	68.29	89.29
External validation		0.842 (0.702–0.933)	80.00	81.82	78.26	78.26	81.82

AUC, area under the curve; CI, confidence interval; PPV, positive predictive value; NPV, negative predictive value.

efficiency was more objective. This study is the first to analyze the value of pleural indentation density changes for predicting VPI. According to the type of contact between the tumor and the pleura, the signs of the related pleural, the characteristics between the tumor and the pleura, and the CT features of the tumor were comprehensively analyzed, the risk factors were explored, and the prediction model was constructed. The results revealed that the AUC value was between 0.842 and 0.862 in the external validation set, indicating a certain level of accuracy.

Previous studies have reported that the pathologic basis of the pleural tags sign may be the compression and closure of the dented visceral pleura due to intrapulmonary pressure, localized edema of the interlobular septum, tumor spread in or outside lymphatic vessels, inflammatory reaction or fibrosis, and focal lobular inflection. Localized

edema of the interlobular septa may be related to lymphatic obstruction. Fibrosis may be caused by the desmoplastic response of the host to the tumor, or it may be associated with a concomitant inflammatory reaction (17-21). For LUAD in direct contact with the pleura, the pleural tags sign was more common in the VPI-positive group. A previous study reported that for LUAD with solid density in direct contact with the pleura, if multiple types of pleural tags signs are combined, the probability of VPI is higher (22), which may be related to the pathological basis of the pleural tags sign. The presence of a pleural tags sign, regardless of its shape, indicates that the reactive fibrosis within the tumor or peritumoral fibrosis is more severe, the tumor is more invasive, and it is more likely to invade the adjacent visceral pleura.

This study found that the pleural indentation sign is an independent risk factor for the occurrence of VPI, irrespective of the direct or indirect contact between the tumor and the pleura, consistent with the findings of previous reports (8,20,21). The mechanism could be that as the tumor grows, the development of reactive fibrous hyperplasia of the tumor, to a certain extent, may cause the adjacent pleura to retract, thereby increasing the risk of visceral pleural invasion. For LUAD with indirect contact with the pleura, type I pleura tags sign (Rat-tail sign) rarely invades the visceral pleura, and type III (Peacock-tail sign) has a higher probability of VPI than type II (Fish-tail sign). This study speculated that the mechanism may be as follows: Line or strip shadows between the tumor and pleura are the visible correlation channels between the tumor and pleura on the CT lung window. In the early stage of tumor development, tumor cells can invade the adjacent pleura through the interstitial components (including lymphatic and blood vessels) in this channel, but they do not cause traction indentation in the adjoining pleura. Consequently, a few type I lesions may have VPI on pathology. When intratumor reactive fibroplasia develops to a certain extent, it may cause adjacent pleural indentation and form type II morphology. The area of adjacent pleural indentation expands as tumor infiltration spreads, forming type III morphology (17).

This study demonstrated that the pleural indentation sign did not differ between the VPI positive and VPI negative groups in the interlobular pleura group, irrespective of the type of contact between the tumor and pleura. The pleural indentation sign in the non-interlobar pleura group was more common in the VPI-positive group than in the VPI-negative group, and the difference was statistically significant. The reason may be that the definition of "pleural indentation sign" in this study is relatively broad. The pleural indentation sign is present as long as the pleura deviates from its normal trajectory. Compared with the costal pleura, diaphragmatic pleura, and mediastinal pleura, the opposite side of the interlobar pleura is an inflated and soft lung tissue. When the intrinsic invasion of the tumor is not enough to invade the visceral pleura, the interlobar pleura can be caused to pull and displace. Consequently, the indentation of the interlobar pleura does not necessarily indicate the occurrence of VPI.

The pleural indentation area revealed on CT is the pleural space between the visceral and parietal pleura and may contain the extrapleural space between the parietal pleura, the inner surface of the rib, and the diaphragm. Microscopically, the extrapleural space contains adipose tissue, loose connective tissue, lymph nodes, blood vessels, internal thoracic fascia, and the most medial intercostal muscle (23). Although the composition is complex, because of the limitation of CT resolution, the pleural area and extrapleural space revealed an intercostal band-like soft tissue density shadow on CT, approximately 1–2 mm thick (24-26). Costal diaphragmatic pleura and mediastinal pleura on CT are difficult to separate. However, the interlobar pleura can be displayed because of the background of the lung. The intercostal banded image combines visceral pleura, parietal pleura, extrapleural adipose tissue, internal thoracic fascia, and the most medial intercostal muscle (23-26). The density of water samples in the indentation pleural area may be due to the displacement of the visceral pleura pulled by the tumor, and the visceral and parietal pleura separated, forming a negative pressure state in the indentation area, which attracted pleural effusion to converge in the indentation area. The indentation area of the pleura is fat density, which may be due to the reactive hyperplasia of adipose tissue in the extrapleural space because of the stimulation of inflammation or tumor. The soft tissue density observed in the pleural indentation area may be attributable to pleural tumor invasion, or it could result from the region of interest being positioned within the internal thoracic fascia and the most medial intercostal muscle in the extrapleural space. This study is the first to analyze the value of pleural indentation density changes in predicting VPI. The results revealed that no matter whether the tumor was in direct or indirect contact with the pleura, analysis of the density changes in the pleural indentation area exhibited no definite guiding significance for predicting the presence or absence of pathological VPI. Whether this

sign has any other differential value must be studied by accurate pathology-imaging comparison.

Based on tumor signs, this study found that the spiculation sign, bronchial change, vascular convergence sign, and emphysema background were related factors for the occurrence of VPI in LUAD through univariate analysis. Spiculation is formed by tumor tissue invading adjacent structures along the surrounding bronchial vascular sheath and lymphatic vessels, and spiculation is an independent risk factor for predicting the invasiveness of LUAD (27). Zhang *et al.* (28) and Liang *et al.* (29) confirmed that bronchial change and vascular convergence sign in GGN were independent risk factors for predicting the invasiveness of LUAD. The appearance of these contractile signs is related to the interstitial infiltration and scar formation of fibroblasts in LUAD. The reactive fibrous hyperplasia increases as the malignancy of the tumor increases, and the traction of adjacent tissues becomes more obvious, resulting in the morphological changes of the bronchi, blood vessels, and pleura in the tumor and its adjoining areas. Previous studies have reported that LUAD with emphysema has more aggressive characteristics and a worse disease-free survival rate than LUAD with a normal lung background (30). Chronic inflammation in chronic obstructive pulmonary disease (COPD) may be a potential key driver of lung cancer aggressiveness (31). LUAD with COPD is more aggressive, so it is more likely to have VPI. The findings of this study are the same as those reported in a previous study (32).

Based on quantitative indicators, this study demonstrated that positive VPI was more common in solid nodules, irrespective of whether the tumor touched the pleura. Additionally, solid component size was an independent risk factor for VPI. The solid component usually represents the more aggressive part of LUAD, a finding consistent with solid component size as a criterion for T staging in clinical staging (33). The larger the maximum size of the solid component, the higher the intrinsic invasiveness of the tumor and the higher the risk of VPI. For LUAD in direct contact with the pleura, this study found that the whole contact pleura length of the lesion and the contact pleura length of the solid components were larger in the VPI-positive group, consistent with the findings of previous studies (10,22). However, inconsistent with Heidinger's study (22), the ratio of whole tumor contact pleural length to tumor size in this study revealed no difference between the two groups, which may be related to the conclusion of solid nodules analyzed separately in Heidinger's study, while the proportion of GGNs included in this study was higher (74.6%). For clinical stage IA LUAD, it is easy to make a misjudgment by only focusing on the ratio of whole lesion contact pleural length to maximum lesion size. This is because the ground glass components primarily represent the area of tumor adherent growth (33), which usually has low invasiveness and is insufficient to penetrate the internal elastane layer of the visceral pleura. It is necessary to focus on whether there are solid components that make contact with the pleura and the maximum size of solid components that make contact with the pleura.

There are limitations to this study. First, this study is a retrospective study with a certain degree of bias in selecting patients. Second, some patients were diagnosed with VPI without accurate pathological grading. Further studies are needed to collect larger samples and patients with accurate pathological grading of VPI. Third, radiomics and deep learning-related research can be performed to explore whether the prediction efficiency of the VPI of such LUAD can be improved.

Conclusions

In conclusion, VPI is one of the poor prognostic factors for clinical stage IA LUAD, and it is an essential factor to consider when choosing the surgical method before surgery. When evaluating whether VPI occurs in clinical stage IA LUAD with pleural contact, attention should be paid to the solid component size. For clinical stage IA LUAD that is in indirect contact with the pleura, when preoperative CT indicates a thick strip-like connection between the tumor and the pleura accompanied by a "Peacock-tail" change in the adjacent pleura indentation, VPI is often indicated. Furthermore, the possibility of VPI should be considered in the context of vascular convergence sign and emphysema background. For LUAD in direct contact with the pleura, attention should be paid to whether there is a pleural tags sign, a solid component touching the pleura, or an indentation in the adjacent pleura. However, it should be noted that interlobar pleura indentation and the density changes in the pleural indentation area do not necessarily indicate VPI. Before the operation, evaluating whether this type of LUAD has an adjacent VPI is beneficial by examining these CT features, which can guide clinical treatment decisions.

Acknowledgments

None.

Footnote

Reporting Checklist: The authors have completed the TRIPOD reporting checklist. Available at https://tcr.amegroups.com/article/view/10.21037/tcr-24-2015/rc

Data Sharing Statement: Available at https://tcr.amegroups.com/article/view/10.21037/tcr-24-2015/dss

Peer Review File: Available at https://tcr.amegroups.com/article/view/10.21037/tcr-24-2015/prf

Funding: This work was supported by the National Key R&D Program of China (Nos. 2022YFC2010000, 2022YFC2010002, 2022YFC2010005), Key Program of National Natural Science Foundation of China (No. 81930049), National Natural Science Foundation of China (Nos. 82171926, 82202140), Shanghai Sailing Program (No. 20YF1449000), Shanghai Science and Technology Innovation Action Plan Program (No. 19411951300), Clinical Innovative Project of Shanghai Changzheng Hospital (No. 2020YLCYJ-Y24), Program of Science and Technology Commission of Shanghai Municipality (No. 21DZ2202600). Special Project for Promoting High-Quality Development of Industries in Shanghai, 2022–2023 (Artificial Intelligence Topic, No. 2023-GZL-RGZN-01014).

Conflicts of Interest: All authors have completed the ICMJE uniform disclosure form (available at https://tcr.amegroups.com/article/view/10.21037/tcr-24-2015/coif). The authors have no conflicts of interest to declare.

Ethical Statement: The authors are accountable for all aspects of the work in ensuring that questions related to the accuracy or integrity of any part of the work are appropriately investigated and resolved. The study was conducted in accordance with the Declaration of Helsinki (as revised in 2013) and approved by the Ethics Committee of the Second Affiliated Hospital of Navy Medical University (No. CZ-20210528-01). The other hospitals were informed and agreed to the study. Individual consent for this retrospective analysis was waived.

References

1. Qi J, Li M, Wang L, et al. National and subnational trends in cancer burden in China, 2005-20: an analysis of national mortality surveillance data. Lancet Public Health 2023;8:e943-55.
2. Goldstraw P, Chansky K, Crowley J, et al. The IASLC Lung Cancer Staging Project: Proposals for Revision of the TNM Stage Groupings in the Forthcoming (Eighth) Edition of the TNM Classification for Lung Cancer. J Thorac Oncol 2016;11:39-51.
3. Inoue M, Minami M, Shiono H, et al. Clinicopathologic study of resected, peripheral, small-sized, non-small cell lung cancer tumors of 2 cm or less in diameter: pleural invasion and increase of serum carcinoembryonic antigen level as predictors of nodal involvement. J Thorac Cardiovasc Surg 2006;131:988-93.
4. Gorai A, Sakao Y, Kuroda H, et al. The clinicopathological features associated with skip N2 metastases in patients with clinical stage IA non-small-cell lung cancer. Eur J Cardiothorac Surg 2015;47:653-8.
5. Yang X, Sun F, Chen L, et al. Prognostic value of visceral pleural invasion in non-small cell lung cancer: A propensity score matching study based on the SEER registry. J Surg Oncol 2017;116:398-406.
6. Zhang T, Zhang JT, Li WF, et al. Visceral pleural invasion in T1 tumors (≤3 cm), particularly T1a, in the eighth tumor-node-metastasis classification system for non-small cell lung cancer: a population-based study. J Thorac Dis 2019;11:2754-62.
7. Wo Y, Zhao Y, Qiu T, et al. Impact of visceral pleural invasion on the association of extent of lymphadenectomy and survival in stage I non-small cell lung cancer. Cancer Med 2019;8:669-78.
8. Sun Q, Li P, Zhang J, et al. CT Predictors of Visceral Pleural Invasion in Patients with Non-Small Cell Lung Cancers 30 mm or Smaller. Radiology 2024;310:e231611.
9. Shi J, Li F, Yang F, et al. The combination of computed tomography features and circulating tumor cells increases the surgical prediction of visceral pleural invasion in clinical T1N0M0 lung adenocarcinoma. Transl Lung Cancer Res 2021;10:4266-80.

10. Ahn SY, Park CM, Jeon YK, et al. Predictive CT Features of Visceral Pleural Invasion by T1-Sized Peripheral Pulmonary Adenocarcinomas Manifesting as Subsolid Nodules. AJR Am J Roentgenol 2017;209:561-6.
11. Zhao Q, Wang JW, Yang L, et al. CT diagnosis of pleural and stromal invasion in malignant subpleural pure ground-glass nodules: an exploratory study. Eur Radiol 2019;29:279-86.
12. Kim HJ, Cho JY, Lee YJ, et al. Clinical Significance of Pleural Attachment and Indentation of Subsolid Nodule Lung Cancer. Cancer Res Treat 2019;51:1540-8.
13. Yang Y, Xie Z, Hu H, et al. Using CT imaging features to predict visceral pleural invasion of non-small-cell lung cancer. Clin Radiol 2023;78:e909-17.
14. Cai X, Wang P, Zhou H, et al. CT-based radiomics nomogram for predicting visceral pleural invasion in peripheral T1-sized solid lung adenocarcinoma. Am J Cancer Res 2023;13:5901-13.
15. Wang F, Pan X, Zhang T, et al. Predicting visceral pleural invasion in lung adenocarcinoma presenting as part-solid density utilizing a nomogram model combined with radiomics and clinical features. Thorac Cancer 2024;15:23-34.
16. Kudo Y, Saito A, Horiuchi T, et al. Preoperative evaluation of visceral pleural invasion in peripheral lung cancer utilizing deep learning technology. Surg Today 2025;55:18-28.
17. Gruden JF. What is the significance of pleural tags? AJR Am J Roentgenol 1995;164:503-4.
18. Hsu JS, Han IT, Tsai TH, et al. Pleural Tags on CT Scans to Predict Visceral Pleural Invasion of Non-Small Cell Lung Cancer That Does Not Abut the Pleura. Radiology 2016;279:590-6.
19. Onoda H, Higashi M, Murakami T, et al. Correlation between pleural tags on CT and visceral pleural invasion of peripheral lung cancer that does not appear touching the pleural surface. Eur Radiol 2021;31:9022-9.
20. Yang S, Yang L, Teng L, et al. Visceral pleural invasion by pulmonary adenocarcinoma ≤3 cm: the pathological correlation with pleural signs on computed tomography. J Thorac Dis 2018;10:3992-9.
21. Qi LP, Li XT, Yang Y, et al. Multivariate Analysis of Pleural Invasion of Peripheral Non-Small Cell Lung Cancer-Based Computed Tomography Features. J Comput Assist Tomogr 2016;40:757-62.
22. Heidinger BH, Schwarz-Nemec U, Anderson KR, et al. Visceral Pleural Invasion in Pulmonary Adenocarcinoma: Differences in CT Patterns between Solid and Subsolid Cancers. Radiol Cardiothorac Imaging 2019;1:e190071.
23. Santamarina MG, Beddings I, Lermanda Holmgren GV, et al. Multidetector CT for Evaluation of the Extrapleural Space. Radiographics 2017;37:1352-70.
24. Vix VA. Extrapleural costal fat. Radiology 1974;112:563-5.
25. Im JG, Webb WR, Rosen A, et al. Costal pleura: appearances at high-resolution CT. Radiology 1989;171:125-31.
26. Hammerman AM, Susman N, Strzembosz A, et al. The extrapleural fat sign: CT characteristics. J Comput Assist Tomogr 1990;14:345-7.
27. Shang X, Hu B, Gao F, et al. Correlation between computed tomography imaging and pathological stages and subtypes in early lung adenocarcinoma. J Cancer Res Ther 2020;16:1569-74.
28. Zhang Y, Qiang JW, Shen Y, et al. Using air bronchograms on multi-detector CT to predict the invasiveness of small lung adenocarcinoma. Eur J Radiol 2016;85:571-7.
29. Liang J, Xu XQ, Xu H, et al. Using the CT features to differentiate invasive pulmonary adenocarcinoma from pre-invasive lesion appearing as pure or mixed ground-glass nodules. Br J Radiol 2015;88:20140811.
30. Lim CG, Shin KM, Lim JK, et al. Emphysema is associated with the aggressiveness of COPD-related adenocarcinomas. Clin Respir J 2020;14:405-12.
31. Parris BA, O'Farrell HE, Fong KM, et al. Chronic obstructive pulmonary disease (COPD) and lung cancer: common pathways for pathogenesis. J Thorac Dis 2019;11:S2155-72.
32. Zuo Z, Li Y, Peng K, et al. CT texture analysis-based nomogram for the preoperative prediction of visceral pleural invasion in cT1N0M0 lung adenocarcinoma: an external validation cohort study. Clin Radiol 2022;77:e215-21.
33. Travis WD, Asamura H, Bankier AA, et al. The IASLC Lung Cancer Staging Project: Proposals for Coding T Categories for Subsolid Nodules and Assessment of Tumor Size in Part-Solid Tumors in the Forthcoming Eighth Edition of the TNM Classification of Lung Cancer. J Thorac Oncol 2016;11:1204-23.

Cite this article as: Lyu D, Wang Y, Tu W, Hu S, Ma Y, Zhou X, Xiao Y, Dong R, Fan L, Liu S. Prediction of visceral pleural invasion of clinical stage IA lung adenocarcinoma based on computed tomography features. Transl Cancer Res 2025;14(3):1596-1608. doi: 10.21037/tcr-24-2015